Time-Efficient Modeling of the Effect of Metal Packages on Electrical Circuits

Zoya Basta Popović and Branko D. Popović

Abstract— **In this work, a method for predicting the effect of conductive plates and boxes on electrical circuit behavior is presented. The method uses the Hallén integral equation to determine currents along circuit branches. The effect of metal packages is taken into account with appropriate images of the circuit branches. Using image theory enables time-efficient approximate full-wave analysis. This approach allows the analysis of circuits placed above a single ground plane, in a metal corner, between parallel metal planes, in rectangular metal pipes or in rectangular metal boxes. The circuits can be made of possibly insulated metal wires and/or narrow strips printed on thin dielectric substrates, and can have lumped generators and lumped or distributed impedances. The method is illustrated on several simple circuit examples and the results are compared to measurements and to results obtained using circuit theory.**

I. Introduction

MICROWAVE and RF circuits often consist of chip elements interconnected by printed strips and vias and are frequently placed in conductive packages, both in digital and analog applications. The effect of these packages at frequencies above a few tens of megahertz on the current distribution along the branches of the circuit cannot be predicted using standard circuit theory. Rigorous electromagnetic field theory using cavity mode expansions [1], [2] can take these effects into account, but is computationally intensive and time consuming. A full-wave analysis, combined with the method of images, was recently used to analyze simple passive circuits [3] and appears to have improved computation time efficiency. On the other hand, some modifications can be made to circuit theory to model circuits in metal enclosures [4], [5] by taking into account a single resonant mode of a closed metal box. Here we present a method for predicting the effect of conductive plates and boxes on circuit behavior above several MHz. The method is a combination of a procedure for solving the Hallén integral equation for current distribution along electrically thin wires and the method of images. It is illustrated on several simple circuit examples and the results are compared to results obtained using circuit theory, as well as to experimental results. A time-efficient Fortran program was used to obtain all results on a 486 33-MHz personal computer.

Manuscript received September 22, 1993; revised April 5, 1994. This work was supported in part by the National Science Foundation under a Presidential Faculty Fellow Award and in part by the Serbian National Research Foundation.

Z. B. Popović is with the University of Colorado, Boulder, CO 80309 USA.
B. D. Popović is with the University of Belgrade, Serbia, Yugoslavia.

IEEE Log Number 9404122.

II. Field Theory Analysis of Circuits in Metal Packages

Circuit theory is based on three implicit assumptions: 1) the current magnitude along any branch is the same along its whole length, 2) the actual size and shape of the circuit elements and interconnecting conductors is irrelevant, and 3) voltages exists only across individual circuit elements. When Kirchhoff's first law is applied to nodes in a circuit, the resulting set of equations is based on assumption 1). Assumptions 2) and 3) are implied when using Kirchhoff's second law. However, these assumptions are exact only in DC circuits. In AC circuits, current intensity is never strictly the same along a branch (due to retardation effects), and distributed voltages exist along all branches (due to varying currents and charges in the entire circuit). Both effects depend on frequency and on the actual size and shape of the circuit, and may become significant even for electrically small circuits. Moreover, if dielectric and/or metal bodies, such as metal packages, are placed near an AC circuit, induced currents and charges in these bodies produce a secondary electric field that influences the behavior of the circuit. All these effects can be analyzed only by means of electromangetic-field theory, and are addressed in this paper.

Among several possibilities [6], the adopted method of analysis in this paper is based on the generalized Hallén-type integral equations [7], [8] and the method of images. The circuit generators and impedances are assumed to be lumped (point-like) and located at one end of the branches. The circuit branches are assumed to be comprised of straight segments. The mathematical model requires the segments to be of circular cross-section, possibly with distributed impedance loading. However, using general quasi-static equivalence, as discussed in detail in [7], insulated wire segments and segments printed on thin dielectric substrates can be transformed into approximately equivalent circular wires with series inductive loading. Therefore, such cases can also be analyzed using the method briefly described below. For narrow strips and strip lines printed on thin dielectric substrates, this is equivalent to an approximation of full-wave analysis.

Consider first a circuit consisting of S arbitrarily interconnected straight segments situated in a homogeneous medium of permittivity ϵ and permeability μ, excited by any number of lumped generators of emfs E_i and angular frequencies ω and containing any number of lumped impedances Z_i ($i = 1, 2, \ldots, S$). Let us concentrate on a single segment, m, of the circuit. Assume that the coordinate axis along the segment is u (with $u = 0$ at one end of the segment), and

the unit vector along the segment is $\mathbf{i}_m$. The branch has an electrically small radius a_m, it is L_m long ($L_m \gg a_m$), and its impedance per unit length is $Z'(u)$. The current magnitude along the segment, $I(u)$, satisfies the following generalized Hallén integral equation [7]

$$j\frac{\mu c}{4\pi}\sum_{n=1}^{S}\int_0^{L_n} I(v)[\mathbf{i}_m\cdot\mathbf{i}_n g(u,v)+G(u,v)]\mathrm{d}v + \int_0^u Z'(s)I(s)\sin\beta(u-s)\mathrm{d}s - B_m\cos\beta u - C_m\sin\beta u = \int_0^u \mathbf{i}_m\cdot\mathbf{E}_i(s)\sin\beta(u-s)\mathrm{d}s, \quad m=1,2,\ldots,S. \tag{1}$$

In this equation, L_n is the length of segment n, v is the coordinate along segment n with the origin at one segment end, B_m and C_m are constants that need to be determined, $G(u,v)$ is given in (5) below, $g(u,v)$ is the Green's function for a homogeneous medium,

$$g(u,v)=e^{(-j\beta R)/R}, \tag{2}$$

where $\beta=\omega/c=\omega\sqrt{\epsilon\mu}$ is the phase coefficient, and

$$R=\sqrt{|\,(\mathbf{r}_m+u\mathbf{i}_m)-(\mathbf{r}_n+v\mathbf{i}_n)\,|^2+a_m^2} \tag{3}$$

is the distance between the source point and the field point. In (3), $\mathbf{r}_m$ is the position vector of the starting-point of segment m, and $\mathbf{r}_n$ is the position vector of the starting-point of segment n. The corresponding scalar-potential, $V(u)$, along segment m is given by [7]

$$V(u) = -B_m\sin\beta u + C_m\cos\beta u + \int_0^u \mathbf{i}_m\cdot\mathbf{E}_i(s)\cos\beta(u-s)\mathrm{d}s - \int_0^u Z'(s)I(s)\cos\beta(u-s)\mathrm{d}s + j\frac{\mu c}{4\pi}\sum_{n=1}^{N}\int_0^{L_n} I(v)F(u,v)\mathrm{d}v. \tag{4}$$

In (1) and (4),

$$G(u,v)=\int_0^u \mathrm{div_{tr}}[\mathbf{i}_n g(s,v)]\cos[\beta(u-s)]\mathrm{d}s,$$
$$F(u,v)=\int_0^u \mathrm{div_{tr}}[\mathbf{i}_n g(s,v)]\sin[\beta(u-s)]\mathrm{d}s. \tag{5}$$

Having in mind that the current along a segment is not the same, we require that Kirchhoff's first law be satisfied at all the nodes of the circuit. For a node with M segments we hence write

$$\sum_{k=0}^{M} I_k(0)=0. \tag{6}$$

The scalar-potential of all the segments connected at the node must be equal at points close to the node, or possibly differ by voltages across point-like generators and/or impedances located at that end of the segments. If we adopt the segment labeled 1 as the reference segment, we can therefore write the following $(M-1)$ conditions for the scalar potential at node m:

$$V_m(0_+)-V_1(0_+)=(E_m-E_1)-[Z_mI_m(0)-Z_1I_1(0)], \quad m=2,\ldots,M. \tag{7}$$

The left-hand side of this equation is computed by means of (4). Therefore, we have a total of M conditions for each node with M segments. It is a simple matter to conclude that for the entire circuit this always results in exactly $2S$ conditions, i.e. two conditions per segment.

For the approximation of the currents along the segments, we adopt polynomials in u, with coefficients I_{mk} to be determined:

$$I(u)=\sum_{k=0}^{D_m} I_{mk}u^k, \quad m=1,2,\ldots,S. \tag{8}$$

The degree of the polynomial approximation in the analysis of circuits is usually $D_m=1$ or $D_m=2$. Note that in circuit theory this degree is implicitly adopted to be zero for all segments.

Finally, the simplest and fastest method for determining the coefficients I_{mk} (and constants B_m and C_m) seems to be the point-matching (collocation) method [10]. According to that method, along every segment we adopt (D_m+1) points (usually equidistant) and stipulate that (1) be satisfied at these points. With the adopted two conditions per segment, this results in a system of linear equations in the unknown parameters I_{mk}, B_m and C_m that can be solved by any suitable numerical method.

Assume now that the circuit is located above a perfectly conducting ground plane. The field of currents and charges induced on the plane is equivalent to that of the image of the circuit in the plane, with the plane removed. Therefore, the solution is the same as for an isolated circuit, except that the Green's function in (1) has two terms: the self-term as in (2), and the term due to the image. The latter must take into account the proper position of the image segment, its reference direction, and the reference direction of the current along it. This current reference direction is opposite to that of the original segment.

The same technique, only resulting in more images, is obtained if the circuit is in a 90 degree metal angle (requiring three images) or in a 90 degree metal corner (requiring seven images). If the circuit is between two parallel metal planes, we first find the image in one plane, then the image of the original circuit and of the first image in the other plane etc., which results in an infinite number of images, as suggested in Fig. 1. Fig. 2 shows images of a circuit branch if it is situated inside a metal tube of rectangular cross-section, from which it is not difficult to visualize images of a circuit inside a rectangular metal box. Naturally, for an approximate solution we can take only a finite number of images in such cases. It will be shown that usually only a few images result in an acceptable solution. The original computer program described in [7] has been extended to enable the analysis of circuits in all described image cases.

Fig. 1. Reference direction of images and the respective currents for a branch between two parallel metal plates.

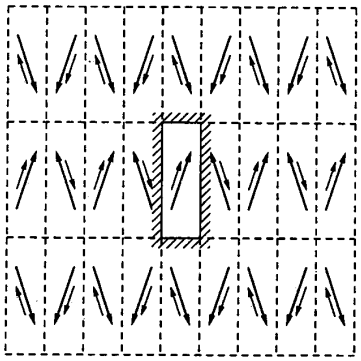

Fig. 2. Reference direction of images and the respective currents for a branch inside a rectangular metal pipe.

It may be worthwhile to point out the principal differences between the field-theory analysis presented in this work (FTA) and circuit-theory analysis (CTA) for solving actual circuits in general, and in the presence of metal packages in particular.

1) The CTA does not, and cannot, take the actual circuit geometry into account, nor the presence of metal packages. Therefore it cannot be used for reliable analysis of circuits at microwave frequencies. The FTA takes these effects into account rigorously.
2) The CTA assumes the AC current along any branch to be the same, while FTA predicts that the current cannot be the same along any single branch. Therefore, for a circuit of N nodes, CTA postulates $(N-1)$ equations according to the first Kirchhoff law, while the FTA requires that these equations be stipulated for all the N nodes.
3) The exact position of a lumped circuit element along a branch in CTA is of no importance, while FTA requires that it be specified.
4) The CTA cannot treat insulated wires or interconnections printed on thin substrates except as short circuits, while FTA considers them as round wires with approximately equivalent distributed inductive loading.
5) The FTA automatically takes into account both the capacitive and inductive coupling between circuit branches. The CTA does not have this capability.

III. Numerical Examples for Some Simple Circuits

The method for determining the effect of metal packages on electrical circuits using images will be first illustrated on the example of a simple low frequency RLC circuit shown in Fig. 3. The circuit is placed in the first octant of the coordinate system, the interconnecting wires are of radius $r = 0.5$ mm, $R_L = 10\ \Omega$, and the reactances of the inductor and capacitor

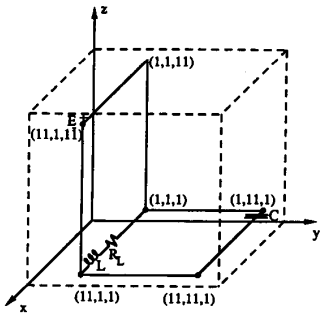

Fig. 3. A resonant circuit is placed in the first quadrant of the coordinate system, where the planes $z = 12$ cm, $y = 12$ cm, and $x = 12$ cm can be metallized. The elements L, C, E and R_L are lumped and are located at segment ends. In the example presented here, $R_L = 10\ \Omega$, and $\omega L = 1/\omega C = 100\ \Omega$ at 10 MHz. The coordinates of nodes, given in parentheses, are in cm.

are both assumed to be 100 Ω at the reference frequency of 10 MHz. In the case of a single metal plane, it is the plane $z = 0$, in case of a 90 degree angle, the planes are $z = 0$ and $y = 0$, and in the case of a metal corner, the plane $x = 0$ is metal as well. When other planes parallel to these are metallized as well, the respective z, y or x coordinates are specified in the input file for the computer program.

The circuit in Fig. 3 was chosen as an example for two reasons. On one hand, this is a very simple circuit in which differences in the field-theory analysis and circuit-theory analysis can be easily illustrated and understood. On the other hand, the effects of metal packages should be more pronounced in resonant circuits. A close metal object is seen by an AC circuit as a short-circuited loop, which alters the circuit inductance and therefore shifts the resonant frequency. Even at low frequency, this example shows considerable effects not predicted by circuit theory, so it becomes evident that circuit theory cannot be used with any certainty at microwave frequencies in such cases.

First consider the circuit without any metal planes present. According to circuit theory, the resonant frequency of the circuit is about $f_{\text{res}} = 9.95$ MHz. At that frequency, the circuit as seen by the generator is an antiresonant circuit (of infinite impedance) in parallel with a resistor of resistance $R = \omega_{\text{res}} L/R_L = 1000\,\Omega$ (approximately).

The field-theory analysis of the circuit, however, yields significantly different results. The resonant frequency is found to be $f'_{\text{res}} = 8.94$ MHz, and the resistance seen by the generator at that frequency to be about $R' = 900\ \Omega$. The shift in resonant frequency can easily be explained by the fact that, in addition to the concentrated inductance L, there is also the intrinsic impedance of the loop (that depends on the loop size and wire diameter) which circuit theory does not take into account. To verify this reasoning, the reactance X of an isolated square loop 0.1 m on a side made of wires with radii $r = 0.05$, 0.5 and 5.0 mm was computed at 10 MHz, using Neumann's formula [11], $X = (-5.03 \ln r - 15.46)\Omega$. In Table 1, this value of X is compared to the value X' obtained using the described numerical method, showing excellent agreement. If this inductance is added to the lumped inductive and

TABLE I
THE RESONANT FREQUENCY OF AN ISOLATED SQUARED LOOP 0.1 m ON THE SIDE, WITH A LUMPED INDUCTOR AND CAPACITOR OF REACTANCES 100 Ω AT 10 MHz, OBTAINED USING CIRCUIT THEORY WITH ADDED LOOP INDUCTANCE (f) AND THE PROPOSED METHOD (f'), VERSUS THE RADIUS, r, OF THE LOOP WIRE. X IS THE INDUCTANCE OF THE LOOP AS CALCULATED FROM NEUMANN'S FORMULA, AND X' THE LOOP INDUCTANCE OBTAINED BY THE PRESENTED METHOD

r (mm)	$X\Omega$ (10 MHz)	$X'\Omega$ (10 MHz)	f (MHz)	f' (MHz)
0.05	34.35	34.34	8.63	8.57
0.50	22.77	22.78	9.02	8.94
5.00	11.19	11.43	9.47	9.33

capacitive reactance of 100 Ω at 10 MHz (with the resistor R_L removed), circuit theory yields significantly lower resonant frequencies than 10 MHz (f in Table 1). These recalculated resonant frequencies are now within 2% of those obtained using the described method (f' in Table 1). In the authors' opinion, f' should be regarded as more accurate than f, because the field-theory analysis approximately includes the stray capacitance across the inductor, as well as other side effects, thus correctly taking into account the shape of the interconnecting wires.

The remaining small difference in the resonant frequency and the difference in the shunt resistance at resonance cannot be explained quantitatively in any simple manner. Note, however, that the vertical loop also has an inductive impedance and that the two loops are significantly magnetically coupled. It is less obvious that the two loops are also electrically coupled by means of the electric field surrounding the concentrated resistance and inductance of the horizontal loop. The method proposed here takes all these electromagnetic effects approximately into account. As a simple illustration, Fig. 4 shows the resistance and reactance of the circuit from Fig. 3 as a function of frequency. Three cases are presented: the circuit in free-space, above a perfectly conducting plane at $z = 0$, and inside a metal box 12 cm on each side. It is clear from these results that the metal planes have a strong effect on the behavior of the circuit. As already pointed out, the presented theory also takes into account the mutual coupling between circuit branches as a function of their *actual* shape, for which circuit theory cannot account. Note that for the circuit above a metal plate and in a metal box the relative difference in resistance can be as large as 10%, and that there is a noticeable difference in the resonant frequency.

Finally, the accuracy of the method with respect to the number of images taken into account was examined. Fig. 5 shows the results for the most computationally intensive case of the circuit in the metal box, at 8.5 MHz, 9.0 MHz and 9.5 MHz. The convergence is seen to be quite rapid, with five pairs of images being evidently sufficient for obtaining results close to the asymptotic values. The results for one frequency point and using 5 pairs of images were obtained on a 486 33 MHz personal computer in less than 25 seconds.

A second example is that of a two-layer printed interconnect circuit with four 22-pF DC blocking capacitors, Fig. 6. The two layers are printed on dielectric substrates 0.5 mm thick with $\epsilon_r = 2.2$. The printed strips of width 0.5 mm on the two layers are interconnected with cylindrical vias 0.3 mm in radius. According to circuit theory, the circuit impedance should

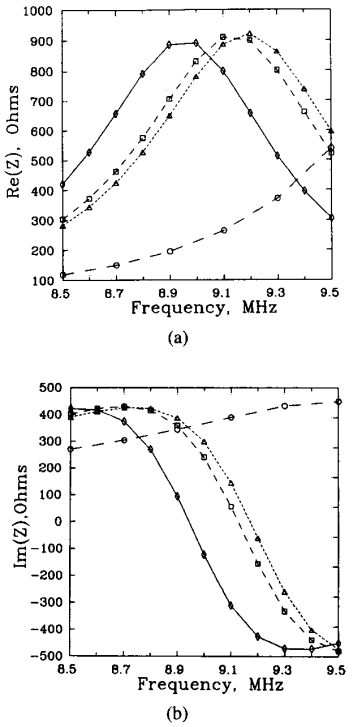

Fig. 4. The resistance (a) and reactance (b) presented to the generator of the circuit from Fig. 3 as a function of frequency. The solid line is for the case of the circuit with no metal planes present, the dashed line corresponds to a single metal plane at $z = 0$, and the dotted line to the circuit placed in a metal box. For comparison, the dashed line with circular symbols shows the curve predicted by standard circuit theory.

always look capacitive and approaches a short circuit with increased frequency. When electromagnetic coupling effects are taken into account, the circuit impedance at 10 MHz varies by about 5% from the reactance of the lumped capacitors, and at 50 MHz the error is more than 70% due to the self and mutual inductances of the circuit loops. Above about 55 MHz the inductive coupling between the circuit branches actually dominates, and at 98 MHz this passive circuit reaches an antiresonance, as shown in Fig. 7 in solid line. The dashed and dotted lines in the same figure show the effects of a single ground plane placed at $z = 0$ and an additional metal plate placed at $z = 2.3$ cm, respectively. The resonant frequency, which was not supposed to exist in the first place, is shifted by more than 10% in the latter case. From this example, it can be seen that the effect of a metal package on passive circuits can be significant, and that it is virtually impossible to predict their broadband behavior without accurate electromagnetic analysis.

The circuit was fabricated on two Rogers' Duroid substrates 0.508 mm thick and with $\epsilon_r = 2.2$. A semi-rigid coaxial cable with a SMA connector was soldered at the place of the lumped generator, and the reflection coefficient of the circuit measured with a HP8702 Network Analyzer (using an electrical/electrical SMA one-port calibration), Fig. 8. For the circuit in free-space, a resonant frequency around 108 MHz with a fairly low Q-factor was measured. As predicted by

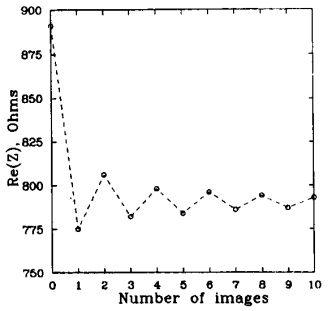

(a)

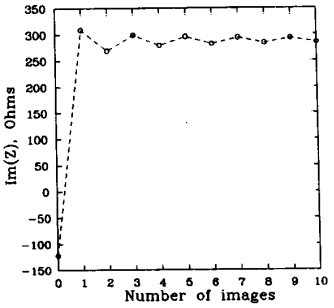

(b)

Fig. 5. The resistance (a) and reactance (b) of the circuit from Fig. 3 at 9.0 MHz, when placed in a metal box, as a function of the number of pairs of images taken into account. The number of images with respect to all planes is the same.

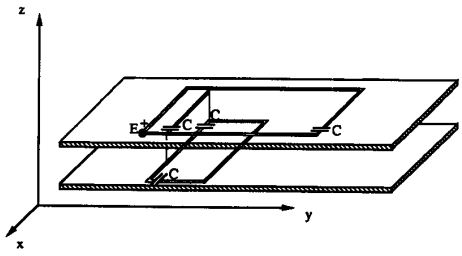

Fig. 6. A two-layer RF interconnect printed circuit with vias and lumped DC blocking capacitors of equal capacitances $C = 22$ pF. The RF signal lines are printed on 0.5-mm thick substrates with $\epsilon_r = 2.2$. The two substrates are 1 and 1.3 cm above the ground plane located at $z = 0$. The size of the top circuit is 5 cm × 7 cm, and that of the lower one is 7 cm × 3 cm. Cylindrical via holes connect the top and bottom substrate metallization. The circuit was analyzed in free-space, above a single perfect ground plane and between two parallel metal plates 2.3 cm apart.

theory, when the circuit is placed 1 cm above a ground plane, the resonance shifts to higher frequencies (112 MHz) and has a larger Q-factor. When a second metal plane is placed in parallel with the first one and 1 cm above the top substrate, the resonance becomes even sharper and shifts up to 115 MHz. Despite the fairly crude fabrication and finite size generator feed, the measured resonances were within less than 10% of the predicted values.

IV. Numerical Example of a Crossover

A simple two-layer crossover is shown in Fig. 9. One of the printed strips is fed from a lumped generator at one end and

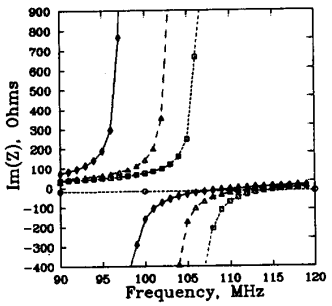

Fig. 7. The computed reactance of the circuit from Fig. 6 between 90 and 120 MHz. The solid line shows results for the circuit in free-space, the dashed line for the circuit above a ground plane at $z = 0$, and the dotted line for the case of a second metal plate at $z = 2.3$ cm. For comparison, the dotted line with circular symbols shows the reactance obtained with just circuit theory.

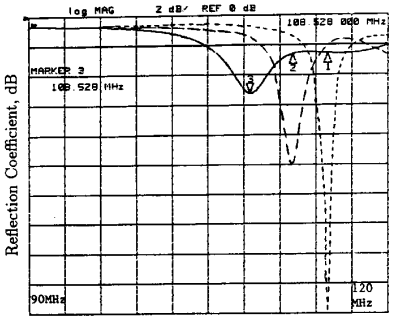

Fig. 8. The measured resonant frequencies of the circuit from Fig. 6 between 90 and 120 MHz. For the circuit in free-space, a resonant frequency around 108 MHz with a fairly low Q-factor was measured (solid line). When the circuit is placed 1cm above a ground plane, the resonance shifts to 112 MHz and has a larger Q-factor (dashed line). When a second metal plane is placed in parallel with the first one and 1 cm above the top substrate, the resonance becomes even sharper and shifts up to 115 MHz (dotted line).

is terminated in a 100 Ω load at the other end. The second line is passive and terminated at both ends in 100 Ω. The two strips of width 1.0 mm are connected with cylindrical vias 0.2 mm in radius and 0.3 and 0.45 cm high to a common ground plane through the loads and generator. The strips are printed on substrates 0.5 mm thick with $\epsilon_r = 2.2$, and are 10 cm long. Two cases are considered: that when the two strips are mutually perpendicular; and when they are parallel, in the same plane.

When the signal and passive strips are perpendicular, there is no magnetic coupling between them, and one might be tempted to conclude that there is no coupling at all. However, since the signal strip is charged, there is capacitive coupling, that results in zero current in the middle of the passive strip and opposite capacitive currents in the two passive strip halves. As a consequence, there are voltages of equal magnitude across the two passive strip terminating resistors. Off course, capacitive coupling as a concept is very well known, but this example shows that the proposed method predicts it properly in a time-efficient manner. Fig. 10(a) shows the voltages across the resistors, for a 1 V generator voltage. Two cases are considered: with and without an additional metal plane parallel

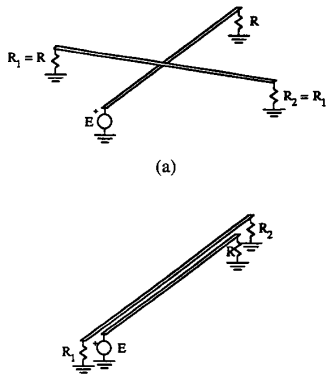

Fig. 9. Sketch of a two-layer crossover. The two printed strips are (a) perpendicular and (b) parallel to each other. One of the printed strips is fed from a lumped generator at one end and is terminated in a 100 Ω load at the other end. The second line is passive and terminated at both ends in 100 Ω. The two strips of width 1.0 mm are connected with cylindrical vias 0.2 mm in radius and 0.3 and 0.45 cm high to a common ground plane through the loads and generator. The strips are printed on substrates 0.5 mm thick with $\epsilon_r = 2.2$, and are 10 cm long.

to the original ground plane, and 0.75 cm above it. It is seen that significant voltages, as high as 15% of the driving voltage, may appear across the resistors terminating the passive strip due to capacitive coupling at high frequencies. It is also seen that the added metal plate has noticeable influence on the voltages and can in some cases reduce the induced voltages.

In the case of parallel strips, there is obviously magnetic coupling. It is less obvious, however, that there is also capacitive coupling, because again the signal strip is charged. As a consequence, different voltages across the two resistors terminating the passive strip should be expected even at frequencies where the strip length is electrically small. Fig. 10(b) shows the voltage across the three resistors of the system without and with the additional metal plate. In this case also, the metal plate has a noticeable influence on circuit behavior.

The theoretical current distribution along the signal and passive line (the horizontal sections only) at 1 GHz is shown in Fig. 11(a) and (b) for perpendicular lines, and in Fig. 11(c) and (d) for parallel lines. These current distributions are calculated for the case when both ground planes are present. For both line sets, the current distribution along the signal line at 10 MHz is practically uniform, but at 1 GHz these distributions are neither uniform nor the same, as illustrated in Fig. 11(a) and (c). The current distribution along the passive line for parallel lines is practically linear and of relatively small magnitude at 10 MHz, but exhibits more complicated behavior and significant magnitude at 1 GHz, as shown in Fig. 11(b) and (d).

V. Conclusion

A method for the analysis of electrical circuits located close to metal planes, or enclosed in metal boxes, is described. The method is a combination of a moment method solution of the generalized Hallén equations and the method of images. The implementation of the method is time efficient. A resonant circuit and a two-level printed interconnect circuit

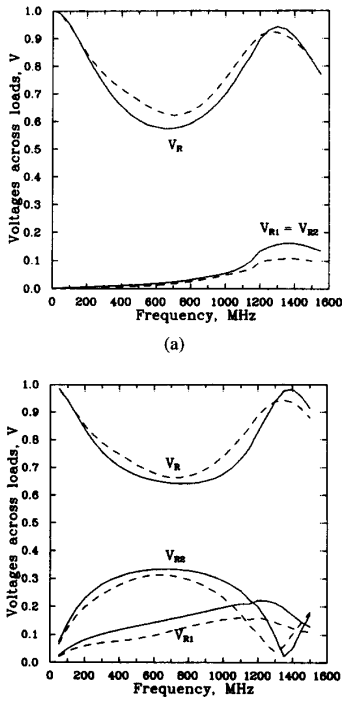

Fig. 10. Voltages across resistors of the circuit sketched in Fig. 9, versus frequency, for a 1 V generator voltage. (a) The case when the printed strips are mutually perpendicular, and (b) when they are parallel. The solid line represents the case with the bottom ground plane present alone, and the dashed line represents the case with an additional ground plane placed 0.75 cm above it.

with DC blocking capacitors are considered as examples of the influence of metal packages on circuits. The first example demonstrates the effects of conductive packages on the resonant frequency of resonant circuits. It is shown that these effects are pronounced even at quite low frequencies on the order of several MHz. The second example demonstrates that the package and circuit shape can result in resonances that should not be present at all according to circuit theory. These results were also experimentally verified. A simple example of a crossover in a package is also considered. The well-known presence of the capacitive coupling was analyzed quantitatively and it was concluded that it can be fairly pronounced in all cases, in contrast to inductive coupling, which, as expected, was not present for the perpendicular crossover.

As a general conclusion, it has been demonstrated that at frequencies above a few MHz electromagnetic theory that takes into account the actual circuit shape and the influence of metal packages is required for accurately predicting circuit behaviour. A time efficient pc-based CAD tool *WireZeus* [6] that has been used for the analysis of isolated electrical circuits and antennas, was modified to enable the analysis of circuits in metal packages. It can deal with the following cases: circuits close to metal plates, right angles or right corners, circuits between parallel metal plates, and circuits inside rectangular

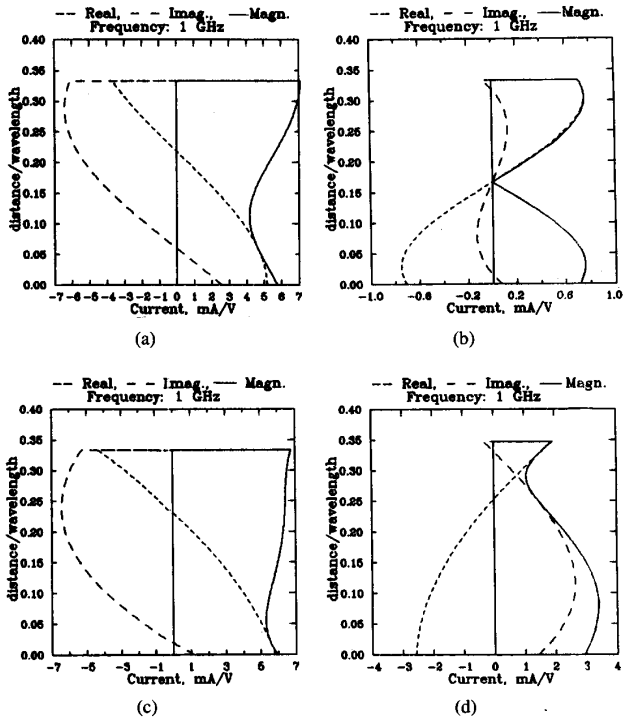

Fig. 11. Real part (dotted line), imaginary part (dashed line) and magnitude (solid line) of current distribution along the signal and passive lines. (a) Signal line and (b) passive line at 1 GHz for perpendicular lines. (c) Signal line and (d) passive line at 1 GHz for parallel lines. The vertical axes are measured along the line in terms of the free-space wavelength, and the horizontal axes in mA per 1 V of the driving voltage. For the signal line, the generator position corresponds to zero distance, and the position of the resistor is where the curves end.

cylindrical pipes or rectangular metal boxes. Since the method is based on an approximation of a full-wave theory, it is valid for practically any frequency of interest, and can give a fast first-order solution to conductive package effects. The paper was intended to be an illustration of this quite general method when applied to packages and interconnects at RF and microwave frequencies.

REFERENCES

[1] J. C. Rautio and R. F. Harrington, "An electromagnetic time-harmonic analysis of shielded microstrip circuits," *IEEE Trans. Microwave Theory Tech.*, vol. MTT-36, pp. 726–730, Aug. 1987.

[2] L. P. Dunleavy and P. B. Katehi, "A generalized method for analyzing shielded thin microstrip discontinuities," *IEEE Trans. Microwave Theory Tech.*, vol. MTT-37, pp. 1758–1766, Dec. 1988.

[3] R. W. Jackson, "The use of side-wall images to compute package effects in MoM analysis of MMIC circuits," *IEEE Trans. Microwave Theory Tech.*, vol. 41, pp. 406–414, Mar. 1993.

[4] R. H. Jensen and L. Wiemer, "Full-wave theory based development of mm-wave circuit models for microstrip open end, gap, step, bend and tee," *IEEE MTT-S Int. Symp. Dig.*, June 1989, pp. 779–782.

[5] J. J. Burke and R. W. Jackson, "A simple circuit model for resonant mode coupling in packaged MMIC's," *IEEE MTT-S Int. Symp. Dig.*, June 1992, pp. 1221–1224.

[6] B. D. Popović, M. B. Dragović, and A. R. Djordjević, *Analysis and Synthesis of Wire Antennas*, Research Studies Press, Ltd. (John Wiley & Sons, Inc.), Chichester–New York, 1982.

[7] B. D. Popović, *CAD of Wire Antennas and Related Radiating Structures.* New York: Wiley, 1991.

[8] B. D. Popović, "Field theory analysis of electrical networks," *Radio Sci.*, vol. 26, pp. 197–202, 1991.

[9] B. D. Popović and A. Nešić, "Generalization of the concept of equivalent radius of thin cylindrical antennas," *Proc. IEE*, vol. 131, Pt. H, no. 3, pp. 153–158, June 1984.

[10] R. F. Harrington, *Field Computation by Moment Methods.* New York: McMillan, 1968.

[11] B. D. Popović, *Introductory Engineering Electromagnetics.* Reading, MA: Addison-Wesley, 1971, pp. 409.

Zoya Basta Popović was born in Belgrade, Yugoslavia, in 1962. She received the Dipl. Ing. degree from the University of Belgrade, Serbia, Yugoslavia and the M.S. and Ph.D. degrees from the California Institute of Technology, Pasadena, in 1985, 1986, and 1990, respectively.

In 1990, she joined the University of Colorado, Boulder, as an Assistant Professor in Electrical Engineering. Her research interests include microwave and millimeter-wave quasi-optical techniques, microwave and millimeter-wave active antennas and circuits and electromagnetic modeling of antennas and circuits.

Dr. Popović received the IEEE MTT 1993 Microwave Prize. Also in 1993, she received the URSI Young Scientist Award and the National Science Foundation Presidential Faculty Fellow Award.

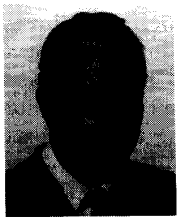

Branko D. Popović received the B.Sc., M.Sc., and D.Sc. degrees from the University of Belgrade, Belgrade, Yugoslavia, in 1958, 1963, and 1967, respectively.

He joined the Department of Electrical Engineering, University of Belgrade in 1959 as a Teaching Assistant, where he served as Assistant Professor, Associate Professor and since 1977 as Professor. He is the author or coauthor of 135 papers in professional journals and proceedings of conferences, six university textbooks, 40 projects dealing with problems in applied electromagnetics (mostly the design of antennas), monographs *Analysis and Synthesis of Wire Antennas* (Wiley, 1982) and *CAD of Wire Antennas and Related Radiating Structures* (Wiley, 1991), and the author of a general program *WireZeus*, for the analysis and design of wire and related antennas.

Dr. Popović was awarded the Heinrich Hertz Premium of the British Institution of Electronic and Radio Engineers (1974), the James Clerk Maxwell Premium of the British Institution of Electronic and Radio Engineers (1985), and the Yogoslav Nikola Tesla Premium (1985), and a number of other awards. He was elected a Corresponding Member of the Serbian Academy of Sciences and Arts in 1978, and a Member of the Academy in 1988.